An Internal Equilibrium Preorganizes the Enzyme−Substrate Complex for Hydride Tunneling in Choline Oxidase†

Fan Fan‡,§ and Giovanni Gadda*,‡,∥,⊥

Departments of Chemistry and Biology and Center for Biotechnology and Drug Design, Georgia State University, Atlanta, Georgia 30302-4098

Received February 6, 2007; Revised Manuscript Received March 20, 2007

ABSTRACT: The hydride transfer reaction catalyzed by choline oxidase under irreversible regime, i.e., at saturating oxygen, was shown in a recent study to occur quantum mechanically within a highly preorganized active site, with the reactive configuration for hydride tunneling being minimally affected by environmental vibrations of the reaction coordinate other than those affecting the distance between the α-carbon of the choline alkoxide substrate and the N(5) atom of the enzyme-bound flavin cofactor [Fan, F., and Gadda, G. (2005) *J. Am. Chem. Soc. 127*, 17954−17961]. In this study, we have determined the effects of pH and temperature on the substrate kinetic isotope effects with 1,2-[$^2H_4$]choline as substrate for choline oxidase at 0.2 mM oxygen to gain insights on the mechanism of hydride transfer under reversible catalytic regime. The data presented indicated that the kinetic complexity arising from the net flux through the reverse of the hydride transfer step changed with temperature, with the hydride transfer reaction becoming more reversible with increasing temperatures. After this kinetic complexity was accounted for, analyses of the k_{cat}/K_m and $^D(k_{cat}/K_m)$ values determined at 0.2 mM according to the Eyring and Arrhenius formalisms suggested that the quantum mechanical nature of the hydride transfer reaction is, not surprisingly, maintained during enzymatic catalysis under reversible regime. A comparison of the thermodynamic and kinetic parameters of the hydride transfer reaction under reversible and irreversible catalytic regimes showed that the enthalpies of activation ($\Delta H^{\ddagger}$) were significantly larger in the reversible catalytic regime. This reflects the presence of an enthalpically unfavorable internal equilibrium of the enzyme−substrate Michaelis complex occurring prior to, and independently from, CH bond cleavage. Such an internal equilibrium is required to preorganize the enzyme−substrate complex for efficient quantum mechanical tunneling of the hydride ion from the substrate α-carbon to the flavin N(5) atom.

Increasing evidence has recently accumulated that implicates environmental enhanced quantum mechanical tunneling in the transfers of hydrogen atoms, protons, and hydride ions in enzymatic oxidations and reductions of organic molecules (for a recent survey of the literature, see refs *1*−*4*). Investigation of coupling of the reaction coordinate to environmental vibrations in the transfer of hydride ions has mainly focused on zinc- and flavin-dependent enzymes that oxidize alcohols to carbonyl compounds, as well as flavin-dependent enzymes that reduce α−β unsaturated carbonyl substrates. Evidence for quantum mechanical transfer of the hydride ion has been obtained for thermophilic alcohol dehydrogenase from *Bacillus stearothermophilus* (*5*−*8*), a mutant form of horse liver alcohol dehydrogenase in which the substitution of an active site residue unmasked the chemical step of hydride transfer (*9*), variant forms of glucose oxidase carrying extensive surface modifications (*10*, *11*), dihydrofolate reductase (*12*−*14*), morphinone reductase (*15*), PETN reductase[1] (*15*), and choline oxidase from *Arthrobacter globiformis* (*16*). A variety of mechanistic approaches have been used in these studies, including temperature-dependent kinetics (*5*−*12*, *15*−*25*), protium−deuterium exchange mass spectrometry (*7*, *23*), and computational studies (*26*−*33*). With the exception of liver alcohol dehydrogenase (*9*), all of the available studies on other enzymes have been carried out under irreversible catalytic regimes to avoid kinetic complexity arising from the chemical step of hydride ion transfer being partially masked by reverse commitments to catalysis (*5*−*8*, *10*−*12*, *15*−*20*, *22*, *23*, *25*). Thus, there is no information to date on the mechanism of hydride ion transfer for enzyme-catalyzed reactions under both reversible and irreversible catalytic regimes.

† This work was supported in part by CAREER Award MCB-0545712 from the National Science Foundation (to G.G.) and a Molecular Basis of Disease Fellowship from Georgia State University (to F.F.).

* To whom correspondence should be addressed at the Department of Chemistry, Georgia State University. Phone: (404) 651-4737. Fax: (404) 651-2751. E-mail: ggadda@gsu.edu.

‡ Department of Biology, Georgia State University.

§ Current address: Biochemistry Department, Albert Einstein College of Medicine, 1300 Morris Park Ave., Bronx, NY 10461.

∥ Department of Chemistry, Georgia State University.

⊥ Center for Biotechnology and Drug Design, Georgia State University.

[1] Abbreviations: PETN reductase, pentaerythritol tetranitrate reductase; $^D(k_{cat}/K_m)$, kinetic isotope effect on the second-order rate constant k_{cat}/K_m with choline as substrate; $^{app}(k_{cat}/K_m)$, apparent second-order rate constant k_{cat}/K_m with choline as substrate determined at subsaturating concentration of oxygen; $^{true}(k_{cat}/K_m)$, true second-order rate constant k_{cat}/K_m with choline as substrate determined at saturating concentration of oxygen.

10.1021/bi700255v CCC: $37.00
Published on Web 05/02/2007

Scheme 1: Minimal Steady-State Kinetic Mechanism of Choline Oxidase[a]

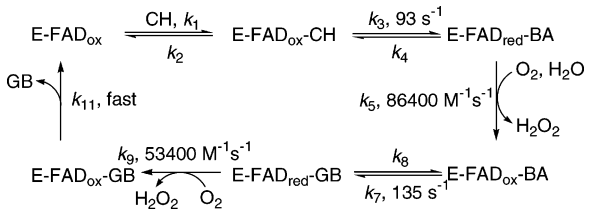

[a] Values for individual rate constants are for pH 10, where kinetic steps are pH-independent (from ref *16*). Abbreviations: E, enzyme; FAD_{ox}, oxidized flavin; FAD_{red}, reduced flavin; CH, choline; BA, betaine aldehyde; GB, glycine betaine.

Choline oxidase (E.C. 1.1.3.17), which catalyzes the flavin-mediated four-electron oxidation of choline to glycine betaine, has been characterized in its biochemical (*34*−*39*) and mechanistic (*16*, *40*−*45*) properties. The enzyme contains FAD in a 1:1 stoichiometry, is a homodimer of 120 kDa (*36*), and under turnover produces a transient betaine aldehyde intermediate that predominantly remains bound at the active site (Scheme 1) (*38*, *41*). The reaction catalyzed by choline oxidase consists of two reductive components in which the enzyme-bound flavin is reduced via the transfer of hydride ions from the alcohol substrate (k_3) and the aldehyde intermediate (k_7), each followed by an oxidative component in which FAD is reoxidized via the transfer of hydride equivalents to molecular oxygen (k_5 and k_9) (*42*). Product release (k_{11}) completes the catalytic cycle. The hydride transfer reaction from the alcohol substrate to the flavin is irreversible when the enzyme is saturated with oxygen (*42*), as suggested by rapid kinetic, pH, and kinetic isotope effect studies (*16*, *42*). This mainly stems from the second-order kinetic step of O_2 reaction with the reduced flavin (k_5) becoming very large when the enzyme is saturated with O_2, which results in negligible concentration of the reduced enzyme−betaine aldehyde Michaelis complex that is required for the reverse hydride transfer reaction under steady-state turnover of the enzyme. In contrast, at concentrations of oxygen smaller than 1 mM the hydride transfer reaction from the alcohol to the enzyme-bound flavin is reversible, as suggested by pH and kinetic isotope effect studies (*16*, *42*).

The elucidation at the molecular level of the catalytic mechanism for alcohol oxidation by choline oxidase has been obtained from pH, temperature, and kinetic isotope effect studies (*16*, *40*, *42*), as well as mutagenesis and mechanistic studies with substrate and product analogues (*37*, *39*, *43*−*45*) (Scheme 2). Catalysis is initiated by deprotonation of the hydroxyl group of the alcohol substrate by an unidentified base with a pK_a of 7.5, which results in the formation of a highly reactive choline−alkoxide species (*42*). The necessary stabilization required for the formation of the alkoxide species is provided by electrostatic interaction with the positive charge of an active site histidine residue, His_{466}, which is fully conserved within members of the glucose−methanol−choline oxidoreductase superfamily to which choline oxidase belongs (*43*). The electrostatic interaction between the choline−alkoxide species and His_{466} also contributes to the positioning of the substrate α-carbon for efficient hydride transfer to the enzyme-bound flavin. Once both activation and correct positioning of the alcohol substrate have been attained in the enzyme active site, the transfer of the hydride ion will occur quantum mechanically by exploiting the environmental vibrations of the reaction coordinate that permit a tunneling distance between the substrate α-carbon and the flavin N(5) atom within the enzyme−substrate complex (*16*).

In the present study, we have investigated the effects of pH and temperature on the kinetic isotope effects with 1,2-[$^2H_4$]choline as substrate for choline oxidase at subsaturating concentration of oxygen, i.e., 0.2 mM, to gain insights on the mechanism of hydride transfer under reversible catalytic regime. The comparison of the mechanistic data presented herein with those previously reported at saturating concentration of oxygen has provided evidence for the presence of an internal equilibrium in the enzyme−substrate Michaelis complex preceding the hydride transfer step. Such an internal equilibrium is required to preorganize the enzyme−substrate complex for efficient quantum mechanical tunneling of the hydride ion from the substrate α-carbon to the flavin N(5) atom. This study provides further understanding of the mechanism of alcohol oxidation catalyzed by enzymatic oxidoreductases and, to a broader extent, of the mechanism of hydride ion tunneling in enzymes with highly preorganized enzyme−substrate configurations.

MATERIALS AND METHODS

Materials. Choline chloride was purchased from ICN. 1,2-[$^2H_4$]Choline bromide (98%) and sodium deuterioxide (99%) were obtained from Isotec Inc. (Miamisburg, OH). Deuterium chloride (99.5%) and deuterium oxide (99.9%) were from Cambridge Isotope Co. (Andover, MA). All other reagents were of the highest purity commercially available. Recombinant choline oxidase from *A. globiformis* strain ATCC 8010 was expressed from plasmid pET/*codA1* and purified to homogeneity as described previously (*36*). The fully oxidized enzyme was prepared as described previously (*37*). All kinetic parameters reported in this study are expressed per active site flavin content.

Enzyme Assays. Enzyme activity was measured polarographically by monitoring initial rates of oxygen consumption with a Hansatech oxygen electrode thermostated at 10−45 °C. Enzyme assays were conducted in 50 mM sodium pyrophosphate, except for pH 7 and 7.5 where potassium phosphate was used. The steady-state kinetic parameters were determined by varying the concentration of choline from 0.02 to 15 mM at a fixed concentration of oxygen of 0.2 mM. The reactions were started by adding choline oxidase at a final concentration of 0.1−0.4 μM into reaction mixtures with a final volume of 1 mL that were previously equilibrated at 0.2 mM oxygen by bubbling the appropriate O_2/N_2 gas mixture for at least 10 min. Substrate deuterium kinetic isotope effects on the steady-state kinetic parameters were determined with choline and 1,2-[$^2H_4$]choline as substrate, by alternating substrate isoptomers.

Data Analysis. Data were fit with KaleidaGraph software (Synergy Software, Reading, PA) and Enzfitter software (Biosoft, Cambridge, U.K.). The steady-state kinetic parameters obtained at fixed concentrations of oxygen were determined by fitting the data to the Michaelis−Menten equation for one substrate. The kinetic isotope effects were then determined by taking the ratios of the steady-state kinetic parameters of interest. The pH dependences of the

Scheme 2: Asynchronous Hydride Transfer Mechanism for Choline Oxidation Catalyzed by Choline Oxidase

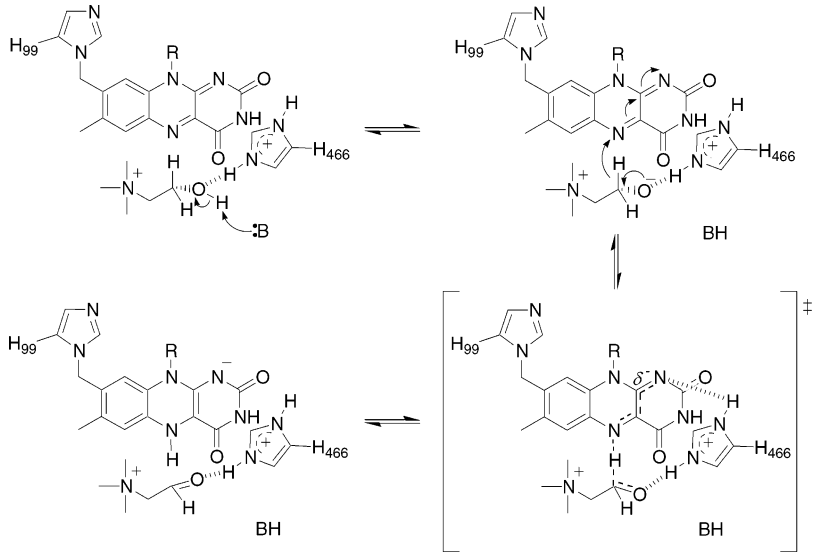

steady-state kinetic parameters were determined by fitting initial rate data to eq 1, which describes a curve with a slope of +1 and a plateau region at high pH. *Y* is the pH-independent value of the kinetic parameter of interest. The pH dependence of the substrate deuterium kinetic isotope effects were determined by fitting initial rate data with eq 2, where Y_L and Y_H are the limiting values at low and high pH, respectively, and K_a is the dissociation constant for the ionization of groups which are relevant to catalysis. The temperature dependences of the steady-state kinetic parameters were determined by fitting initial rate data with the Eyring equation (eq 3), where k_B and *h* are the Boltzmann and Planck constants, respectively. The enthalpy of activation ($\Delta H^{\ddagger}$) is calculated from the slope of the plot, whereas the entropy ($\Delta S^{\ddagger}$) is calculated from *y*-intercept of the plot. The temperature dependences of the deuterium kinetic isotope effects were determined by fitting the data with the Arrhenius equation (eq 4), where A_H/A_D is the isotope effect on the preexponential factors and $[E_a(D) - E_a(H)]$ is the isotope effect on the energy of activation.

$$\log Y = \log\left[\frac{Y}{1 + (10^{-pH}/10^{-pK_a})}\right] \quad (1)$$

$$\log Y = \log\left[\frac{Y_L + Y_H(10^{-pK_a}/10^{-pH})}{1 + (10^{-pK_a}/10^{-pH})}\right] \quad (2)$$

$$\ln[(k_{cat}/K_m)/T] = \ln(k_B/h) + \Delta S^{\ddagger}/R - \Delta H^{\ddagger}/RT \quad (3)$$

$$\ln(\mathrm{KIE}) = \ln[A_H/A_D] - [E_a(D) - E_a(H)]/RT \quad (4)$$

RESULTS AND DISCUSSION

Temperature Dependence of Kinetic Isotope Effects at Subsaturating Oxygen. Recent pH and kinetic isotope effect studies established that oxygen availability determines whether the reduced enzyme−betaine aldehyde complex partitions forward to catalysis during turnover with choline rather than reverting to the oxidized enzyme−choline alkoxide complex (*42*). At saturating oxygen, oxidation of choline is irreversible, and the resulting $^{D}(k_{cat}/K_m)$ value approaches the intrinsic kinetic isotope effect between pH 5 and pH 10 (*16*, *42*). At concentrations of oxygen ≤1 mM, choline oxidation becomes progressively more reversible with decreasing $[O_2]$ due a significant increase of the reverse commitment to catalysis, which in the minimal mechanism of Scheme 1 is defined by the ratio $k_4/k_5[O_2]$ (*16*). A recent study reported the effect of temperature on the $^{D}(k_{cat}/K_m)$ and k_{cat}/K_m values with choline at saturating oxygen concentrations as a probe for the involvement of quantum mechanical tunneling in the reaction of hydride transfer catalyzed by choline oxidase (*16*). In the present study, we have expanded that investigation and determined the effect of temperature on the $^{D}(k_{cat}/K_m)$ and k_{cat}/K_m values at subsaturating concentration of oxygen to gain further insights on the mechanism of hydride tunneling under reversible catalytic regime.

Initial rates of reaction were measured over temperatures ranging from 10 to 45 °C at varying concentrations of choline and 1,2-[$^2H_4$]choline and at a fixed concentration of oxygen of 0.2 mM and pH 8 (Table S1 of the Supporting Information). As shown in Figure 1A, the analysis of the data according to the Eyring formalism showed that the k_{cat}/K_m values with both isoptomers increased monotonically with increasing temperature, yielding slopes that were larger with 1,2-[$^2H_4$]choline than with choline. The Arrhenius analysis of the temperature dependence of the resulting kinetic isotope effects showed that the $^{D}(k_{cat}/K_m)$ values increased with decreasing temperature (Figure 1B). These data are in stark contrast with results previously reported on choline oxidase obtained at saturating oxygen concentration, showing similar slopes for the k_{cat}/K_m values with choline and 1,2-[$^2H_4$]choline and a temperature-independent $^{D}(k_{cat}/K_m)$ value of ~10.6 (*16*). The different patterns observed at saturating and nonsaturating concentrations of oxygen may stem from either a change in the quantum tunneling contribution to hydride transfer under irreversible and reversible catalytic regimes or a temperature effect on the kinetic complexity of the reaction catalyzed by the enzyme.

Determination of Kinetic Complexity at Subsaturating Oxygen. In the reaction catalyzed by choline oxidase (Scheme 1) kinetic complexity can potentially arise from an increased partitioning of the reduced enzyme−betaine aldehyde complex between the reverse of the hydride transfer reaction (k_4)

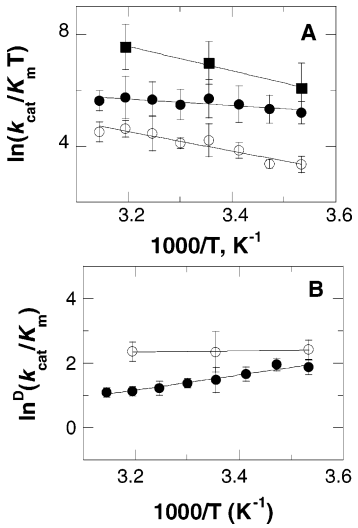

FIGURE 1: Temperature dependences of the k_{cat}/K_m and $^D(k_{cat}/K_m)$ values with choline at subsaturating $[O_2]$. Panel A: $(k_{cat}/K_m)/T$ values with (●) choline, (○) 1,2-[$^2H_4$]choline, and (■) choline after correction for kinetic complexity. Panel B: $^D(k_{cat}/K_m)$ values before (●) and after (○) correction for kinetic complexity. Kinetic parameters were determined at 0.2 mM oxygen in 50 mM sodium pyrophosphate, pH 8. Data were fit to eq 3 (panel A) and eq 4 (panel B).

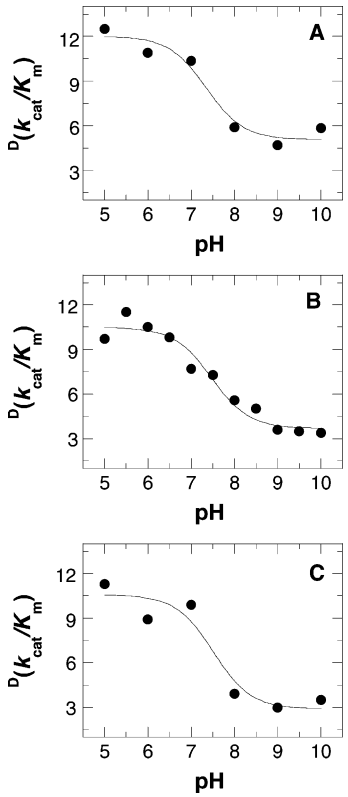

FIGURE 2: pH dependence of the $^D(k_{cat}/K_m)$ values with choline and 1,2-[$^2H_4$]choline at subsaturating $[O_2]$ determined at 10 °C (panel A), 25 °C (panel B), and 40 °C (panel C). Kinetic parameters were measured at a fixed concentration of 0.2 mM oxygen [or 0.25 mM oxygen for the data at 25 °C (*16*)]. Data were fit to eq 2.

and reaction with O_2 ($k_5[O_2]$), an increased partitioning of the oxidized enzyme−choline complex between hydride transfer reaction (k_3) and dissociation of the substrate from the enzyme active site (k_2), or both. In this regard, previous solvent viscosity and substrate kinetic isotope effects with choline, as well as pH studies on glycine betaine inhibition and with the choline analogues *N*,*N*-dimethylethanolamine and *N*-methylethanolamine as substrate for the enzyme, unequivocally established choline as a slow substrate for choline oxidase, for which $k_2 \gg k_3$ (*37*, *38*, *42*). Consequently, any kinetic complexity must necessarily arise from the partitioning of the reduced enzyme−betaine aldehyde complex between the reverse of the hydride transfer reaction and the reaction with O_2, i.e., from the $k_4/k_5[O_2]$ ratio.

In order to establish whether the kinetic complexity of the reaction catalyzed by choline oxidase at subsaturating concentration of oxygen changed with temperature, the effect of pH on the $^D(k_{cat}/K_m)$ values measured at 0.2 mM oxygen was determined at three selected temperatures spanning over 10−40 °C (Table S2 of the Supporting Information). As shown in Figure 2, the $^D(k_{cat}/K_m)$ values decreased between limiting values with increasing pH in all cases. The limiting $^D(k_{cat}/K_m)$ values at low pH were 11.2 ± 0.6 at 10 °C, 10.5 ± 0.4 at 25 °C, and 10.6 ± 0.9 at 40 °C, in reasonable agreement with the intrinsic $^D(k_{cat}/K_m)$ value of ∼10.6 that was previously determined at saturating oxygen and 25 °C (*42*). In contrast, the limiting $^D(k_{cat}/K_m)$ values at high pH progressively decreased with increasing temperature, with values of 5.1 ± 0.6 at 10 °C, 3.7 ± 0.4 at 25 °C, and 2.9 ± 0.9 at 40 °C, consistent with $k_4/k_5[O_2]$ ratios with increasing temperatures. The kinetic complexity (C_r) at any given temperature was then estimated by using eq 5, where $^D(k_{cat}/K_m)$ represents the observed kinetic isotope effect determined at high pH and 0.2 mM oxygen, and $^Dk_3$ and ^{D}Eq are the intrinsic kinetic and equilibrium isotope effect for the hydride transfer reaction, respectively. A reasonable approximation of the $^Dk_3$ value is provided by the pH-independent value of 10.6 previously determined for the $^D(k_{cat}/K_m)$ value at saturating oxygen concentration (*42*), which is in excellent agreement with the limiting $^D(k_{cat}/K_m)$ values determined at low pH in this study at 0.2 mM oxygen (Figure 2), at which kinetic complexity is expected to be negligible. A ^{D}Eq value of 1.24, which was previously established by Cleland for the conversion of alcohols to aldehydes (*46*), can be used for the equilibrium isotope effect for conversion of choline to betaine aldehyde. By using the limiting $^D(k_{cat}/K_m)$ values at high pH determined in this study, $k_4/k_5[O_2]$ ratios of 1.4 ± 0.4, 2.8 ± 0.5, and 5.1 ± 1.9 were then estimated at 10, 25, and 40 °C, suggesting that at 0.2 mM oxygen the hydride transfer reaction catalyzed by choline oxidase becomes progressively more reversible as a function of temperature.

$$^D\left(\frac{k_{cat}}{K_m}\right) = \frac{^Dk_3 + 1.24C_r}{1 + C_r} \qquad \text{with } C_r = \frac{k_4}{k_5[O_2]} \qquad (5)$$

In the steady-state kinetic mechanism of choline oxidase (Scheme 1), the $^{app}(k_{cat}/K_m)$ value for choline determined at subsaturating oxygen concentrations comprises rate constants reflecting substrate binding (k_1 and k_2), the chemical step of hydride transfer from choline to the flavin in the forward and reverse directions (k_3 and k_4), and the kinetic step in which the reduced enzyme−betaine aldehyde complex reacts with molecular oxygen (k_5), as shown in eq 6. Choline being a slow substrate for the enzyme (*37*, *38*, *45*) is consistent with $k_2 \gg k_3$, resulting in the measured k_{cat}/K_m value determined at any given subsaturating concentration of oxygen being an $^{app}(k_{cat}/K_m)$ value, as illustrated in eq 7. In

Table 1: Thermodynamic Parameters on k_{cat}/K_m Values for Oxidation of Choline by Choline Oxidase at 0.2 mM and Saturating Concentrations of Oxygen[a]

[oxygen], mM	0.2	saturating[b]
$\Delta H^{\ddagger}_{H}$,[c] kJ mol^{-1}	29 ± 4[d]	18 ± 2
$\Delta H^{\ddagger}_{D}$,[c] kJ mol^{-1}	30 ± 4	18 ± 5
$-T\Delta S^{\ddagger}_{H}$,[c] kJ mol^{-1}	34 ± 8[d]	24 ± 2
$-T\Delta S^{\ddagger}_{D}$,[c] kJ mol^{-1}	19 ± 2	30 ± 5
$\Delta S^{\ddagger}_{H}$,[e] kJ mol^{-1}	0.11 ± 0.03	0.08 ± 0.01
$\Delta S^{\ddagger}_{D}$,[e] kJ mol^{-1}	0.06 ± 0.01	0.10 ± 0.02
$\Delta G^{\ddagger}_{H}$,[e] kJ mol^{-1}	63 ± 10[d]	42 ± 5
$\Delta G^{\ddagger}_{D}$,[e] kJ mol^{-1}	49 ± 6	48 ± 13
ΔE_a,[e] kJ mol^{-1}	0.4 ± 0.3	0.4 ± 4.2
A_H/A_D[f]	6 ± 1	11 ± 8
KIE	10.5 ± 0.4	10.6 ± 0.6

[a] Conditions: 50 mM sodium pyrophosphate, pH 8. [b] Data are from ref *16*. [c] Data were calculated using the Eyring equation. [d] Data with choline at 0.2 mM oxygen after correction for the contribution of the reverse commitment to catalysis. [e] Data for 25 °C. [f] Data were calculated using the Arrhenius equation.

contrast, at saturating oxygen concentrations, at which the $k_4/k_5[O_2]$ ratio approaches a negligible value and thereby C_r approaches zero, the measured k_{cat}/K_m values equal k_1k_3/k_2 and represent $^{true}(k_{cat}/K_m)$ values. This analysis establishes a direct correlation between the $^{app}(k_{cat}/K_m)$ values that are determined at subsaturating concentrations of oxygen, the kinetic complexity of the enzymatic reaction (C_r), and the $^{true}(k_{cat}/K_m)$ values (eq 8). By using eq 8 and the C_r values determined from the pH profiles of the $^{D}(k_{cat}/K_m)$ values determined at 0.2 mM oxygen and different temperatures, the true k_{cat}/K_m values with choline at pH 8 after correction for the kinetic complexity could be estimated with values of 124000 ± 21000, 340000 ± 37000, 598000 ± 63000 at 10, 25, and 40 °C, respectively.

$$^{app}\left(\frac{k_{cat}}{K_m}\right) = \frac{k_1k_3}{k_2(1 + C_r) + k_3} \quad (6)$$

$$^{app}\left(\frac{k_{cat}}{K_m}\right) = \frac{k_1k_3}{k_2(1 + C_r)} \quad (7)$$

$$^{true}\left(\frac{k_{cat}}{K_m}\right) = {}^{app}\left(\frac{k_{cat}}{K_m}\right)(1 + C_r) \qquad \text{with} \quad {}^{true}\left(\frac{k_{cat}}{K_m}\right) = \frac{k_1k_3}{k_2} \quad (8)$$

Eyring and Arrhenius Analyses of the Temperature Effects at 0.2 mM Oxygen after Correction for Kinetic Complexity. After correction for kinetic complexity an Eyring analysis of the k_{cat}/K_m values with choline and 1,2-[$^2H_4$]choline at 0.2 mM oxygen showed similar slopes for the two isoptomers (Figure 1A), consistent with similar enthalpies of activation ($\Delta H^{\ddagger}$) with values of ~30 kJ mol^{-1} for the cleavages of the CH and CD bonds of choline. Thus, the entire kinetic isotope effect associated with the transfer of the hydride ion in the reaction catalyzed by choline oxidase has an entropic rather than an enthalpic origin. The entropy of activation at 25 °C ($\Delta S^{\ddagger}$) was less than 0.1 kJ mol^{-1} with both the light and heavy isotopes, in agreement with the values previously reported at saturating oxygen (Table 1) (*42*). The Arrhenius analysis of the $^{D}(k_{cat}/K_m)$ values at subsaturating concentration of oxygen corrected for kinetic complexity yielded a temperature-independent kinetic isotope effect of ~10.5 (Figure 1B), which compared well with the pH-independent $^{D}(k_{cat}/K_m)$ value of ~10.6 reported in previous studies at saturating oxygen (Table 1) (*42*). In agreement with the $^{D}(k_{cat}/K_m)$ values being temperature-independent, the ΔE_a value determined at 0.2 mM oxygen was negligible (Table 1). Finally, within the accuracy of the analysis, the isotope effect on the Arrhenius preexponential factors (A_H/A_D) was not significantly different from the $^{D}(k_{cat}/K_m)$ value (Table 1), further consistent with an entropic origin of the kinetic isotope effect that is associated with the hydride transfer reaction in choline oxidase.

The thermodynamic parameters on the k_{cat}/K_m values for oxidation of choline at 0.2 mM oxygen, after correction for kinetic complexity, are consistent with the hydride transfer reaction occurring through environmentally enhanced quantum mechanical tunneling within a highly preorganized enzyme−substrate complex (*16*). This conclusion is supported by the temperature-independent $^{D}(k_{cat}/K_m)$ value, the similar values for the isotope effect on the Arrhenius preexponential factors A_H/A_D and the $^{D}(k_{cat}/K_m)$ value, and the similarities in the enthalpies of activation ($\Delta H^{\ddagger}$) with finite values that are larger than zero for the light and heavy isoptomers of choline (*7*, *9*, *15*, *20*, *22*, *47*). Indeed, a classical over-the-barrier mechanism for hydride transfer can be ruled out from the A_H/A_D value being significantly larger than 1.7 (*48*), whereas H^- and D^- tunneling just below the classical transition state is not consistent with the similar finite $\Delta H^{\ddagger}$ values for CH and CD bond cleavage and the lack of temperature effects on the $^{D}(k_{cat}/K_m)$ value (*49*, *50*). Moreover, the temperature independence of the $^{D}(k_{cat}/K_m)$ suggests that the probability of H^- and D^- transfer is similar at different temperatures, consistent with minimal dynamical motions of the enzyme−substrate complex other than those associated with the subpicosecond vibration of the CH bond along the reaction coordinate that promote the tunneling of the hydride ion (*2*, *4*, *16*). This, in turn, is consistent with the active site in the choline alkoxide−choline oxidase Michaelis complex being highly preorganized to facilitate the quantum mechanical transfer of the hydride from the activated substrate to the enzyme-bound flavin.

An Internal Equilibrium Preorganizes the Substrate−Enzyme Complex for Subsequent Hydride Ion Tunneling. The results presented in this study, along with the results recently reported for the temperature effects on the $^{D}(k_{cat}/K_m)$ values determined at saturating oxygen concentration (*16*), establish that the hydride transfer reaction catalyzed by choline oxidase occurs quantum mechanically both under reversible and under irreversible catalytic regimes. The lack of temperature dependence of the $^{D}(k_{cat}/K_m)$ values is further consistent with a highly preorganized active site in the choline alkoxide−choline oxidase Michaelis complex that undergoes hydride transfer (*1*, *9*, *13*, *15*−*20*, *22*, *47*, *49*, *51*, *52*), with little independent movements of the substrate α-carbon and flavin N(5) atom other than those resulting in the quantum mechanical tunneling of the hydride ion. This implies that any environmental organization of the enzyme−substrate complex that is necessarily required to bring the hydride donor and acceptor in a preorganized configuration suitable for tunneling of the hydride ion must occur prior to, and in a fashion that is mechanistically uncoupled to, the hydride transfer reaction. In this context, while most of the thermodynamic parameters for the hydride transfer reaction are, within the accuracy of the determinations, independent of

Scheme 3: Proposed Preorganization of the Enzyme−Substrate Michaelis Complex in Choline Oxidase[a]

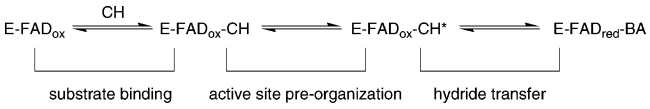

[a] Abbreviations: E, enzyme; FAD_{ox}, oxidized flavin; FAD_{red}, reduced flavin; CH, choline; BA, betaine aldehyde.

whether the reaction occurs in reversible or irreversible catalytic regimes (Table 1), the enthalpies of activation ($\Delta H^{\ddagger}$) for CH and CD bond cleavage under reversible catalytic regime are significantly larger than those determined in irreversible catalytic regime, i.e., ~30 kJ mol^{-1} versus ~18 kJ mol^{-1}. These differences are consistent with the presence of an enthalpically unfavorable internal equilibrium of the enzyme−substrate Michaelis complex occurring prior to and independently from the CH bond cleavage reaction (Scheme 3). From a mechanistic standpoint, the environmental preorganization of the enzyme−substrate complex is probably associated with, or perhaps simply triggered by, the deprotonation reaction of the hydroxyl group of the alcohol substrate that results in the formation of the activated choline alkoxide species (Scheme 2). Indeed, the cleavage of the substrate OH bond has been previously demonstrated to occur prior to the subsequent hydride transfer reaction by using solvent and substrate kinetic isotope effects (*42*).

Conclusions. The results of the mechanistic investigation on the effects of temperature and pH on the kinetic isotope effects with deuterated choline presented in this study established that the quantum mechanical character of the hydride transfer reaction of alcohol oxidation catalyzed by choline oxidase is, not surprisingly, maintained when the catalytic regime of the reaction shifts from irreversible to reversible. Under both catalytic regimes, the hydride ion tunnels from the α-carbon of the activated choline alkoxide species to the enzyme-bound flavin N(5) atom within a highly preorganized enzyme−substrate complex, with little independent movements of the hydride donor and acceptor other than those conducive to tunneling of the hydride ion. Thus, choline oxidase has evolved to maximize productive binding of the alcohol substrate so that in the enzyme−substrate complex all of the components of the catalytic machinery, i.e., the catalytic base that activates the substrate (*16*, *38*, *40*), the positive charge that stabilizes the resulting alkoxide species (*39*, *43*), and the isoalloxazine ring of the flavin (*36*), are properly positioned to exploit the mechanical effects that result in the transfer of the hydride ion from the substrate α-carbon to the flavin N(5) atom. The comparison of the data obtained in reversible and irreversible catalytic regimes has unveiled for the first time the presence of an enthalpically unfavorable internal equilibrium occurring in the choline oxidase−substrate complex prior to the hydride transfer reaction. The internal equilibrium is required to preorganize the enzyme−substrate complex for efficient quantum mechanical tunneling of the hydride ion. In this respect, the conformational change that allows the preorganization of the active site for the subsequent tunneling of the hydride ion in choline oxidase is temporarily and mechanistically distinct from the protein dynamical effects resulting in hydride tunneling that occur after formation of the competent enzyme−substrate complex. Thus, choline oxidase represents the first instance of an enzymatic hydride tunneling reaction from a highly preorganized active site in which the necessary preorganization of the active site in the enzyme−substrate complex has been observed experimentally. This study therefore represents the first example of the use of temperature-dependent kinetic isotope effects to measure thermodynamic parameters for hydride ion tunneling that are associated with the presence of conformational changes occurring in the enzyme−substrate complex. This approach is particularly effective for those cases in which the conformational changes are not detectable by using other approaches because they are kinetically fast, as for the case of choline oxidase. To date, several cases for enzymatic reactions involving tunneling of hydride ions, protons, and hydrogen atoms from highly preorganized active sites have been proposed (*7*, *8*, *16*, *47*, *53*). It is expected that by using an approach similar to that used in this study conformational changes that preorganize the active site will be unveiled in a growing number of enzymes.

ACKNOWLEDGMENT

The authors thank Drs. Judith P. Klinman, Vern L. Schramm, Justine P. Roth, Tom Netzel, and John S. Blanchard for discussion and insightful suggestions.

SUPPORTING INFORMATION AVAILABLE

Two tables showing (i) the apparent kinetic parameters with choline and 1,2-[$^2H_4$]choline as substrate for choline oxidase determined at 0.2 mM oxygen and pH 8 in the temperature range from 10 to 45 °C and (ii) the apparent kinetic parameters with choline and 1,2-[$^2H_4$]choline as substrate for choline oxidase determined at 0.2 mM oxygen at 10 or 45 °C in the pH range from 5 to 10. This material is available free of charge via the Internet at http://pubs.acs.org.

REFERENCES

1. Klinman, J. P. (2006) The role of tunneling in enzyme catalysis of C-H activation, *Biochim. Biophys. Acta 1757*, 981−987.
2. Masgrau, L., Roujeinikova, A., Johannissen, L. O., Hothi, P., Basran, J., Ranaghan, K. E., Mulholland, A. J., Sutcliffe, M. J., Scrutton, N. S., and Leys, D. (2006) Atomic description of an enzyme reaction dominated by proton tunneling, *Science 312*, 237−241.
3. Nagel, Z. D., and Klinman, J. P. (2006) Tunneling and dynamics in enzymatic hydride transfer, *Chem. Rev. 106*, 3095−3118.
4. Sutcliffe, M. J., Masgrau, L., Roujeinikova, A., Johannissen, L. O., Hothi, P., Basran, J., Ranaghan, K. E., Mulholland, A. J., Leys, D., and Scrutton, N. S. (2006) Hydrogen tunnelling in enzyme-catalysed H-transfer reactions: flavoprotein and quinoprotein systems, *Philos. Trans. R. Soc., London 361*, 1375−1386.
5. Kohen, A., Cannio, R., Bartolucci, S., and Klinman, J. P. (1999) Enzyme dynamics and hydrogen tunnelling in a thermophilic alcohol dehydrogenase, *Nature 399*, 496−499.
6. Kohen, A., and Klinman, J. P. (2000) Protein flexibility correlates with degree of hydrogen tunneling in thermophilic and mesophilic alcohol dehydrogenase, *J. Am. Chem. Soc. 122*, 10728−10729.
7. Liang, Z. X., Lee, T., Resing, K. A., Ahn, N. G., and Klinman, J. P. (2004) Thermal-activated protein mobility and its correlation with catalysis in thermophilic alcohol dehydrogenase, *Proc. Natl. Acad. Sci. U.S.A. 101*, 9556−9561.
8. Liang, Z. X., Tsigos, I., Bouriotis, V., and Klinman, J. P. (2004) Impact of protein flexibility on hydride-transfer parameters in thermophilic and psychrophilic alcohol dehydrogenases, *J. Am. Chem. Soc. 126*, 9500−9501.
9. Rubach, J. K., Ramaswamy, S., and Plapp, B. V. (2001) Contributions of valine-292 in the nicotinamide binding site of liver alcohol

dehydrogenase and dynamics to catalysis, *Biochemistry 40*, 12686−12694.
10. Kohen, A., Jonsson, T., and Klinman, J. P. (1997) Effects of protein glycosylation on catalysis: changes in hydrogen tunneling and enthalpy of activation in the glucose oxidase reaction, *Biochemistry 36*, 2603−2611.
11. Seymour, S. L., and Klinman, J. P. (2002) Comparison of rates and kinetic isotope effects using PEG-modified variants and glycoforms of glucose oxidase: the relationship of modification of the protein envelope to C-H activation and tunneling, *Biochemistry 41*, 8747−8758.
12. Maglia, G., and Allemann, R. K. (2003) Evidence for environmentally coupled hydrogen tunneling during dihydrofolate reductase catalysis, *J. Am. Chem. Soc. 125*, 13372−13373.
13. Sikorski, R. S., Wang, L., Markham, K. A., Rajagopalan, P. T., Benkovic, S. J., and Kohen, A. (2004) Tunneling and coupled motion in the *Escherichia coli* dihydrofolate reductase catalysis, *J. Am. Chem. Soc. 126*, 4778−4779.
14. Kim, H. S., Damo, S. M., Lee, S. Y., Wemmer, D., and Klinman, J. P. (2005) Structure and hydride transfer mechanism of a moderate thermophilic dihydrofolate reductase from *Bacillus stearothermophilus* and comparison to its mesophilic and hyperthermophilic homologues, *Biochemistry 44*, 11428−11439.
15. Basran, J., Harris, R. J., Sutcliffe, M. J., and Scrutton, N. S. (2003) H-tunneling in the multiple H-transfers of the catalytic cycle of morphinone reductase and in the reductive half-reaction of the homologous pentaerythritol tetranitrate reductase, *J. Biol. Chem. 278*, 43973−43982.
16. Fan, F., and Gadda, G. (2005) Oxygen- and temperature-dependent kinetic isotope effects in choline oxidase: correlating reversible hydride transfer with environmentally enhanced tunneling, *J. Am. Chem. Soc. 127*, 17954−17961.
17. Agrawal, N., Hong, B., Mihai, C., and Kohen, A. (2004) Vibrationally enhanced hydrogen tunneling in the *Escherichia coli* thymidylate synthase catalyzed reaction, *Biochemistry 43*, 1998−2006.
18. Basran, J., Patel, S., Sutcliffe, M. J., and Scrutton, N. S. (2001) Importance of barrier shape in enzyme-catalyzed reactions. Vibrationally assisted hydrogen tunneling in tryptophan tryptophylquinone-dependent amine dehydrogenases, *J. Biol. Chem. 276*, 6234−6242.
19. Basran, J., Sutcliffe, M. J., and Scrutton, N. S. (1999) Enzymatic H-transfer requires vibration-driven extreme tunneling, *Biochemistry 38*, 3218−3222.
20. Basran, J., Sutcliffe, M. J., and Scrutton, N. S. (2001) Deuterium isotope effects during carbon-hydrogen bond cleavage by trimethylamine dehydrogenase. Implications for mechanism and vibrationally assisted hydrogen tunneling in wild-type and mutant enzymes, *J. Biol. Chem. 276*, 24581−24587.
21. Battaile, K. P., Molin-Case, J., Paschke, R., Wang, M., Bennett, D., Vockley, J., and Kim, J. J. (2002) Crystal structure of rat short chain acyl-CoA dehydrogenase complexed with acetoacetyl-CoA: comparison with other acyl-CoA dehydrogenases, *J. Biol. Chem. 277*, 12200−12207.
22. Harris, R. J., Meskys, R., Sutcliffe, M. J., and Scrutton, N. S. (2000) Kinetic studies of the mechanism of carbon-hydrogen bond breakage by the heterotetrameric sarcosine oxidase of *Arthrobacter* sp. 1-IN, *Biochemistry 39*, 1189−1198.
23. Liang, Z. X., Tsigos, I., Lee, T., Bouriotis, V., Resing, K. A., Ahn, N. G., and Klinman, J. P. (2004) Evidence for increased local flexibility in psychrophilic alcohol dehydrogenase relative to its thermophilic homologue, *Biochemistry 43*, 14676−14683.
24. Rubach, J. K., and Plapp, B. V. (2003) Amino acid residues in the nicotinamide binding site contribute to catalysis by horse liver alcohol dehydrogenase, *Biochemistry 42*, 2907−2915.
25. Tsai, S., and Klinman, J. P. (2001) Probes of hydrogen tunneling with horse liver alcohol dehydrogenase at subzero temperatures, *Biochemistry 40*, 2303−2311.
26. Agarwal, P. K., Webb, S. P., and Hammes-Schiffer, S. (2000) Computational studies of the mechanism for proton and hydride transfer in liver alcohol dehydrogenase, *J. Am. Chem. Soc. 122*, 4803−4812.
27. Caratzoulas, S., Mincer, J. S., and Schwartz, S. D. (2002) Identification of a protein-promoting vibration in the reaction catalyzed by horse liver alcohol dehydrogenase, *J. Am. Chem. Soc. 124*, 3270−3276.
28. Hammes-Schiffer, S. (2001) Theoretical perspectives on proton-coupled electron transfer reactions, *Acc. Chem. Res. 34*, 273−281.
29. Hammes-Schiffer, S. (2002) Comparison of hydride, hydrogen atom, and proton-coupled electron transfer reactions, *ChemPhysChem 3*, 33−42.
30. Hammes-Schiffer, S. (2002) Impact of enzyme motion on activity, *Biochemistry 41*, 13335−13343.
31. Hammes-Schiffer, S. (2004) Quantum-classical simulation methods for hydrogen transfer in enzymes: a case study of dihydrofolate reductase, *Curr. Opin. Struct. Biol. 14*, 192−201.
32. Hammes-Schiffer, S., and Iordanova, N. (2004) Theoretical studies of proton-coupled electron transfer reactions, *Biochim. Biophys. Acta 1655*, 29−36.
33. Masgrau, L., Basran, J., Hothi, P., Sutcliffe, M. J., and Scrutton, N. S. (2004) Hydrogen tunneling in quinoproteins, *Arch. Biochem. Biophys. 428*, 41−51.
34. Ohishi, N., and Yagi, K. (1979) Covalently bound flavin as prosthetic group of choline oxidase, *Biochem. Biophys. Res. Commun. 86*, 1084−1088.
35. Ikuta, S., Imamura, S., Misaki, H., and Horiuti, Y. (1977) Purification and characterization of choline oxidase from *Arthrobacter globiformis*, *J. Biochem. (Tokyo) 82*, 1741−1749.
36. Fan, F., Ghanem, M., and Gadda, G. (2004) Cloning, sequence analysis, and purification of choline oxidase from *Arthrobacter globiformis*: A bacterial enzyme involved in osmotic stress tolerance, *Arch. Biochem. Biophys. 421*, 149−158.
37. Gadda, G., Powell, N. L., and Menon, P. (2004) The trimethylammonium headgroup of choline is a major determinant for substrate binding and specificity in choline oxidase, *Arch. Biochem. Biophys. 430*, 264−273.
38. Ghanem, M., Fan, F., Francis, K., and Gadda, G. (2003) Spectroscopic and kinetic properties of recombinant choline oxidase from *Arthrobacter globiformis*, *Biochemistry 42*, 15179−15188.
39. Ghanem, M., and Gadda, G. (2006) Effects of reversing the protein positive charge in the proximity of the flavin N(1) locus of choline oxidase, *Biochemistry 45*, 3437−3447.
40. Gadda, G. (2003) pH and deuterium kinetic isotope effects studies on the oxidation of choline to betaine-aldehyde catalyzed by choline oxidase, *Biochim. Biophys. Acta 1650*, 4−9.
41. Gadda, G. (2003) Kinetic mechanism of choline oxidase from *Arthrobacter globiformis*, *Biochim. Biophys. Acta 1646*, 112−118.
42. Fan, F., and Gadda, G. (2005) On the catalytic mechanism of choline oxidase, *J. Am. Chem. Soc. 127*, 2067−2074.
43. Ghanem, M., and Gadda, G. (2005) On the catalytic role of the conserved active site residue His466 of choline oxidase, *Biochemistry 44*, 893−904.
44. Fan, F., Germann, M. W., and Gadda, G. (2006) Mechanistic studies of choline oxidase with betaine aldehyde and its isosteric analogue 3,3-dimethylbutyraldehyde, *Biochemistry 45*, 1979−1986.
45. Gadda, G., Fan, F., and Hoang, J. V. (2006) On the contribution of the positively charged headgroup of choline to substrate binding and catalysis in the reaction catalyzed by choline oxidase, *Arch. Biochem. Biophys. 451*, 182−187.
46. Cleland, W. W. (1980) Measurement of isotope effect by the equilibrium perturbation technique, in *Methods in Enzymology* (Purich, D. L., Ed.) pp 104−125, Academic Press, New York.
47. Knapp, M. J., Rickert, K., and Klinman, J. P. (2002) Temperature-dependent isotope effects in soybean lipoxygenase-1: correlating hydrogen tunneling with protein dynamics, *J. Am. Chem. Soc. 124*, 3865−3874.
48. Bell, R. P. (1974) Liversidge Lecture. Recent advances in the study of kinetic hydrogen isotope effects, *Chem. Soc. Rev.*, 513−544.
49. Knapp, M. J., and Klinman, J. P. (2002) Environmentally coupled hydrogen tunneling. Linking catalysis to dynamics, *Eur. J. Biochem. 269*, 3113−3121.
50. Kohen, A., and Klinman, J. P. (1998) Enzyme catalysis: beyond classical paradigms, *Acc. Chem. Res. 31*, 397−404.
51. Kohen, A., and Klinman, J. P. (1999) Hydrogen tunneling in biology, *Chem. Biol. 6*, R191−198.
52. Scrutton, N. S., Basran, J., and Sutcliffe, M. J. (1999) New insights into enzyme catalysis—ground state tunneling driven by protein dynamics, *Eur. J. Biochem. 264*, 666−671.
53. Agarwal, P. K., Billeter, S. R., Rajagopalan, P. T., Benkovic, S. J., and Hammes-Schiffer, S. (2002) Network of coupled promoting motions in enzyme catalysis, *Proc. Natl. Acad. Sci. U.S.A. 99*, 2794−2829.

BI700255V